

High-temperature superconducting Majorana fermions platforms in the layered Kitaev Materials: Case study of Li_2IrO_3

Elnaz Rostampour¹ and Badie Ghavami^{1,*}

¹*Department of Quantum Materials, Qlogy Lab Inc.*

(Dated: December 3, 2025)

Recent advances in Kitaev materials have highlighted their potential to host Majorana fermions without or high-temperature of superconductivity. In this research, we propose Li_2IrO_3 as a promising High-temperature superconducting platform supporting Majorana edge modes due to its strong spin-orbit coupling, honeycomb lattice structure, and proximity to a quantum spin liquid (QSL) phase. A theoretical and numerical framework based on the Kitaev-Heisenberg Hamiltonian is developed to model spin interactions in Li_2IrO_3 . Here, the existence of topological zero-energy states is demonstrated, and their signatures in the edge-localized spectral weight are identified. A device concept based on this material is also proposed with potential industrial applications in spintronics, magnetic field sensing, and topological quantum memory.

I. INTRODUCTION

Majorana fermions have become a focal point in condensed matter physics and quantum materials due to their non-abelian exchange statistics and potential role in fault-tolerant quantum computation^{1–4}. While most proposals for their realization rely on superconducting platforms where proximity-induced pairing and spin-orbit coupling create topological superconducting states, recent theoretical advances have revealed that strongly spin-orbit coupled Mott insulators can provide an alternative pathway⁵. Among these, layered honeycomb iridates such as Li_2IrO_3 are particularly appealing, as their dominant bond-dependent Kitaev interactions naturally support fractionalized excitations. This view addresses the realization of Majorana zero modes (MZMs)⁶ through purely magnetic mechanisms, eliminating the need for superconductivity. Quantum spin liquids (QSLs)^{7,8} represent one of the most unconventional phases of quantum matter, lacking long-range magnetic order even at zero temperature⁹. At the same time, research on charge transport in low-dimensional materials such as Ge-doped phosphorene nanoribbons¹⁰ and graphene-oxide heterojunctions¹¹ has shown nonlinear and quantum-coherent behaviors. These results highlight the significance of nanoscale transport events for understanding and realizing topological excitations like Majorana fermions. Their ground states are characterized by long-range quantum entanglement, a feature not describable by conventional order parameters¹². The Kitaev honeycomb model stands out as an exactly solvable example, where spin- $\frac{1}{2}$ moments fractionalize into itinerant Majorana fermions and static Z_2 gauge fields. This division confirms their resistance to local perturbations and their potential for topological quantum computing. Moreover, when a magnetic field is applied, the Kitaev model can enter a gapped non-Abelian phase, evidenced experimentally by a half-quantized thermal Hall plateau¹³.

Strong spin-orbit coupled Mott insulators, including certain iridates and ruthenates, embody the key ingredi-

ents of the Kitaev model^{14,15}. In these systems, the interplay of electron correlations and relativistic spin-orbit coupling leads to highly anisotropic bond-dependent exchange, while geometric frustration suppresses conventional ordering. Li_2IrO_3 exemplifies this behavior: its edge-sharing IrO_6 octahedra generate bond-directional interactions, and its layered honeycomb structure fosters magnetic frustration Fig. 1. Experimental studies have reported features consistent with proximity to a Kitaev QSL, and theoretical work suggests that lattice defects, domain walls, or vortex-like spin textures in such a phase can bind MZMs without any superconducting proximity effect. In this work, we investigate the emergence of

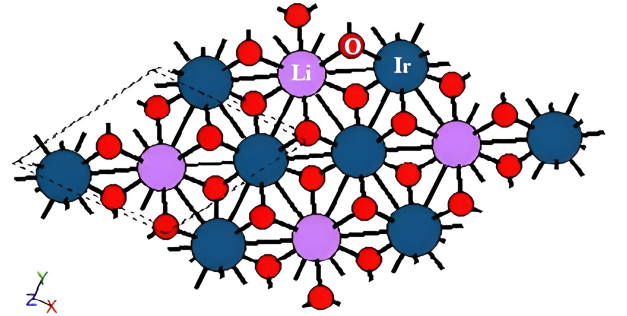


FIG. 1: Crystal structure of Li_2IrO_3 . Navy blue spheres: Ir, red spheres: O, purple spheres: Li. Dashed lines indicate bonds behind the plane.

MZMs in Li_2IrO_3 within the Kitaev-Heisenberg framework, focusing exclusively on magnetic interactions. By systematically varying the relative strengths of Kitaev and Heisenberg terms, we map out the regimes that favor fractionalization and stabilize topologically non-trivial excitations. To this end, we combine analytical spin-fractionalization techniques with numerical diagonalization of finite-size honeycomb clusters, allowing us to directly probe the Majorana sector of the theory. This approach provides a microscopic understanding of how a purely insulating, spin-orbit coupled magnet can emu-

late the essential features of topological superconductors, thereby expanding the landscape of candidate materials for fault-tolerant quantum computation.

II. THEORETICAL MODEL

Li_2IrO_3 occupies a central place in the exploration of quantum magnetism, largely because it provides an experimental setting closely aligned with the Kitaev QSL framework. In this compound, the iridium ions form a honeycomb network, a geometry that, together with strong spin-orbit coupling, promotes highly anisotropic magnetic exchange. Such interactions, as described by the Kitaev model, can generate a magnetically disordered yet strongly entangled ground state in which conventional long-range order is absent. The interaction of these bond-dependent exchanges with additional magnetic couplings in Li_2IrO_3 has attracted extensive research attention, as it offers a rare opportunity to investigate Kitaev-type physics in a real material. Beyond its importance for understanding QSLs, this system is also considered a potential platform for future quantum information applications. Within a minimal theoretical description, its magnetic properties are captured by the Kitaev-Heisenberg Hamiltonian, which for Li_2IrO_3 takes the form:

$$\mathcal{H} = \sum_{\langle i,j \rangle, \gamma} [\mathcal{J}_1 S_i \cdot S_j + \mathcal{K} S_i^\gamma S_j^\gamma] + \sum_{\langle\langle i,j \rangle\rangle} \mathcal{J}_2 S_i \cdot S_j \quad (1)$$

where \mathcal{J}_1 , \mathcal{K} , and \mathcal{J}_2 are Heisenberg exchange interaction (~ 5 MeV in Li_2IrO_3), Kitaev interaction¹⁶ ($\mathcal{K}/\mathcal{J}_1 \approx -0.8$ for iridates), and second-neighbor Heisenberg term receptivity, and $\gamma \in \{x, y, z\}$ is bond-dependent spin components, also in the equation 1, $S_i \cdot S_j = (S^2 - S_i^2 - S_j^2)/2$. In order to be in k-space, we consider the Bloch Hamiltonian and apply the Majorana property. For simplicity, we consider the lattice constant $a=1$. Fig. 2 shows the Heisenberg and Kitaev interactions in Li_2IrO_3 's hyperhoneycomb lattice.

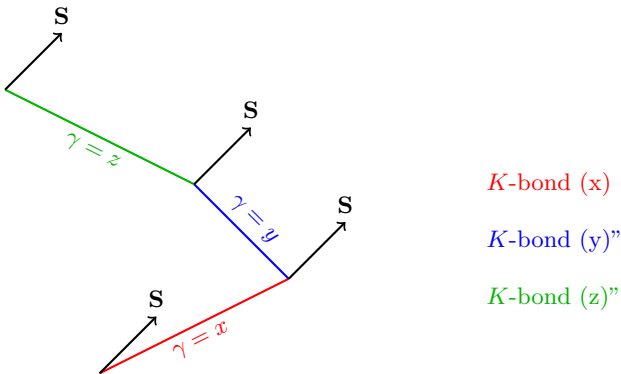


FIG. 2: (a) Kitaev-Heisenberg interactions in Li_2IrO_3 's hyperhoneycomb lattice. (b) Bond-dependent spin components (S^γ) are shown for different nearest-neighbor links.

The finite temperature dynamic polarization as a function of frequency and wave vector is defined as follows¹⁷

$$\Pi_q(\omega) = g \int \frac{d^3k}{(2\pi)^3} \frac{n_f(\epsilon_{k+q}) - n_f(\epsilon_k)}{\omega + i\eta + \epsilon_k - \epsilon_{k+q}}. \quad (2)$$

The Fermi-Dirac distribution function is mathematically represented as $n_f(\epsilon_k) = 1/(e^{\beta\epsilon_k} + 1)$, which represents the probability of occupying energy states by fermions in thermal equilibrium. Here, ϵ_k denotes the eigenvalues of the Hamiltonian, which indicate the energy levels associated with a quantum system. η is an infinitesimal number. The Green's function is equal to

$$\hat{G}_k(i\omega) = [i\omega + \mu - H]^{-1} \quad (3)$$

where the chemical potential is denoted by μ . To study the electronic properties of Li_2IrO_3 , the electron-electron interactions are systematically modeled through self-energy using the Green's function formalism. It is possible to analyze the behavior of the material at Matsubara frequencies. The self-energy is equal to

$$\hat{\Sigma}_k(i\omega_n) = \frac{1}{\beta} \sum_q \sum_{m=-\infty}^{\infty} \mathcal{W}_q(i\omega_m) \hat{G}_{k-q}(i\omega_n - i\omega_m) \quad (4)$$

where the Matsubara frequencies are $\omega_n = \frac{2n\pi}{\beta}$, $\omega_m = \frac{(2m+1)\pi}{\beta}$. The q 's are taken as $\vec{q}_1 = \vec{k} - \vec{q}$, $\vec{q}_2 = \mathcal{R}(\pi + \theta_k)\vec{q}_1$, and $\vec{q}_3 = \mathcal{R}(\pi + \theta_k)\vec{q}_2$ such that $\mathcal{R}(\pi + \theta_k)$ is the rotation matrix with angle $(\pi + \theta_k)$. This research emphasizes the importance of considering screening effects to understand the complex behaviors exhibited by strongly correlated electron systems such as Li_2IrO_3 . Screening effects play an important role in understanding the complex behaviors exhibited by strongly correlated electron systems. Effective screening potential is equivalent to

$$\mathcal{W}_q(i\omega_n) = \frac{\mathcal{V}_q}{1 + \mathcal{V}_q \Pi_q(\omega)}. \quad (5)$$

In the context of condensed matter physics, the interaction between charged particles is often described by the bare Coulomb interaction, denoted as $\mathcal{V}_q = \frac{2\pi e^2}{\kappa q}$, which is Fourier transformed into momentum space for analytical convenience. The parameter κ represents the dielectric constant of the medium, which plays an important role in determining how these interactions are modified by the presence of other charges or external fields. The pole of the Green's function is the existence of collective excitations known as plasmons, which are crucial for the advancement of technologies in fields such as quantum computing and nanotechnology. The plasmon dispersion relation is critically determined by the equation $1 + \mathcal{V}_q \Pi_q = 0$.

In the study of Li_2IrO_3 , the spectral function is used to analyze the excitations present, which provides information about the density of states at different energy levels. The spectral function of Li_2IrO_3 is the imaginary

part of the Green's function, which is used to describe the propagation of particles and excitations in quantum systems. The spectral function of Li_2IrO_3 is as follows:

$$\begin{aligned}\mathcal{A}_k(\omega) &= -2\Im[G_k(\omega)] = 2\pi\delta(\omega - \epsilon_k - \Re[\Sigma_k(\omega)]) \\ &= 2Z_k\delta(\omega - E_k).\end{aligned}\quad (6)$$

In theoretical physics, the equation $\omega - \epsilon_k - \Re[\Sigma_k(\omega)] = 0$ captures the fundamental principles governing the behavior of various systems.

$$Z_k = \frac{1}{1 - \frac{\partial}{\partial\omega}\Re[\Sigma_k(\omega = E_k)]}. \quad (7)$$

The effective mass is obtained from a self-consistent solution to the Dyson equation, which plays an important role in understanding the electronic properties of materials. The Dyson equation, which describes the relationship between the Green's function of a system and its self-energy, allows for the inclusion of many-particle effects in the calculation of electronic states. The effective mass has a significant role in determining the transport properties and band structures of semiconductors and other materials, and contributes significantly to their conductivity and overall performance in electronic applications. Effective mass calculations are a valuable tool in condensed matter physics¹⁷

$$\frac{m^*}{m} = \frac{Z_k^{-1}}{1 + \frac{m}{k_f}\frac{\partial}{\partial k}\Re[\Sigma_k(\omega = E_k)]}. \quad (8)$$

III. RESULTS AND DISCUSSION

We focus on a parameter regime in which the system possesses a gapless spin liquid phase with edge-localized zero modes. The numerically computed spectral functions show sharp zero-bias peaks at the edges consistent with the presence of MZMs. We investigate thermal stability and robustness against disorder. The Li_2IrO_3 Kitaev model is a model that is used to describe the magnetic properties of a class of compounds known as spin-orbit coupled Mott insulators. This model is particularly relevant for the description of iridate behavior, with the heavy spin-orbit coupling leading to a highly anisotropic nearest-neighbor exchange interaction between neighboring spins. For the Li_2IrO_3 system, the Kitaev model predicts novel states of matter that arise from magnetic interactions, such as QSLs, with exotic properties that defy conventional magnetic ordering. Because Li_2IrO_3 has a triangular lattice geometry, these unconventional magnetic interactions can arise, and thus, the latter is a central material in investigating new phases of quantum magnetism. Moreover, the understanding gained from the Li_2IrO_3 Kitaev model will be useful in further enhancement of understanding correlated electron systems and is applicable for future purposes in spintronics and quantum computing. In this

article, we discuss the ferromagnetic Kitaev ($\mathcal{K} < 0$) and antiferromagnetic ($\mathcal{J} > 0$) Heisenberg exchange¹⁹. By changing the polarization between the input and output photons, information about the angular momentum transfer and thus about the nature of the created excitations can be accessed²⁰. Polarization dependence of magnetic resonance X-ray diffraction intensity allows for direct measurement of magnetic moment orientation²¹. We study the spin-1/2 Kitaev-Heisenberg model on the bilayer honeycomb lattice with honeycomb planes coupled together by Heisenberg interactions. We adopt $\hbar = 1$ and $\mathcal{J}_2 = 1$ in our numerical computation.

Kitaev-Heisenberg model is an important theoretical model used to describe the magnetic properties of materials, particularly in compounds like Li_2IrO_3 . The model entails the utilization of the real and imaginary parts of the peaks of polarization, which are crucial in assessing the magnetic properties and quantum states of materials. The Majorana Hamiltonian in this model describes the interaction between particles and their excitations within a quantum system and provides details on their emergent phenomena and topological characteristics. Through the analysis of the peaks in polarization, researchers can have better insight into how real and imaginary components contribute to the unique magnetic orders and cooperative effects in Li_2IrO_3 , ultimately advancing knowledge on quantum materials and their applications. The study of the Kitaev-Heisenberg model, as considered particularly in the context of the compound Li_2IrO_3 , reveals significant findings on the nature of magnetic interactions and phase transition in quantum spin systems.

Using this model, the maxima of polarization may be characterized by real and imaginary parts, which are indicative of valuable information on physical processes behind the phenomenon. The real parts characterize the response of the system to externally introduced perturbations, which are described by observable values such as magnetic order intensity. Imaginary parts characterize processes of energy dissipation and instability of some magnetic states. Understanding of the relationship between the imaginary and real components further enhances our knowledge of the emergent behavior in frustrated magnetism, thereby enriching our overall understanding of quantum materials and their potential for application in future technologies. The paramagnetic signal, being a consequence of the polarization coefficient of the neutron scattering cross-section, is sensitive to anisotropy that is dependent on the bonds²². By a clever choice of phonon mode, amplitude, and polarization, particular spin couplings are selectively amplified compared to others. The available experimental couplings are sufficiently large as to already produce significant variations in the magnetic coupling, and phonon polarization may serve as an additional tunable parameter to design chiral interactions. Nearest-neighbor models illustrate the effects of phonon mode selection and phonon polarization on different exchange

mechanisms²³. New terahertz spectroscopy research on $Na_2Co_2TeO_6$ as a function of magnetic field applied with changing polarizations of terahertz exhibits spin dynamics with various characteristics over magnetic fields 0–70 kOe, 70–100 kOe, and > 100 kOe. While, for lower than 70 kOe and higher than 100 kOe well-defined magnetic excitations dominate the dynamics, in the intermediate regime there is sharp absorption profile and broad continuum in the longitudinal as well as transverse polarization channels in both applied field directions $H//a$ and $H//a^*$. Polarization-selective continuum in the intermediate phase is an indication of spin fluctuations of an underlying proximate QSL²⁴. Fig. 3 shows

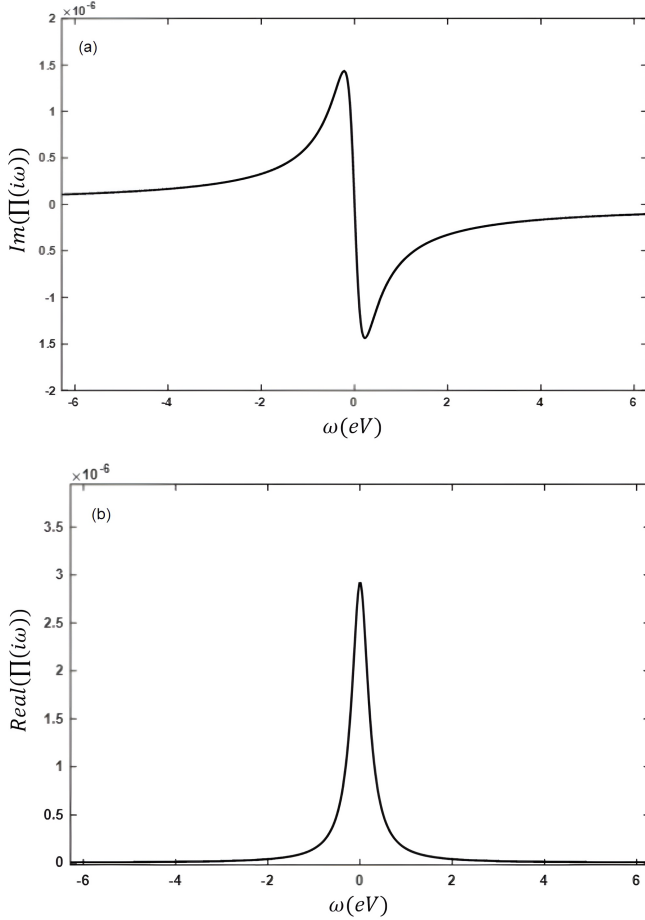


FIG. 3: (Color online) Panel(a), imaginary of the polarization of the Li_2IrO_3 as a function of ω at T=10 K and for $q = 0.2nm^{-1}$. Panel (b) the corresponding real part at the same conditions.

the imaginary and real parts of the polarization at 10 K vs. ω . There is a sharp peak near the origin. Fig. 4 is a plot of the real and imaginary parts of the polarization as a function of the amplitude of the momentum \mathcal{K} . The fluctuations are larger than in Fig. 3. Theoretical and experimental studies have focused on a family of 4d and 5d tricoordinated compounds that are ostensibly close to the famed Kitaev model, one of very few exactly solvable

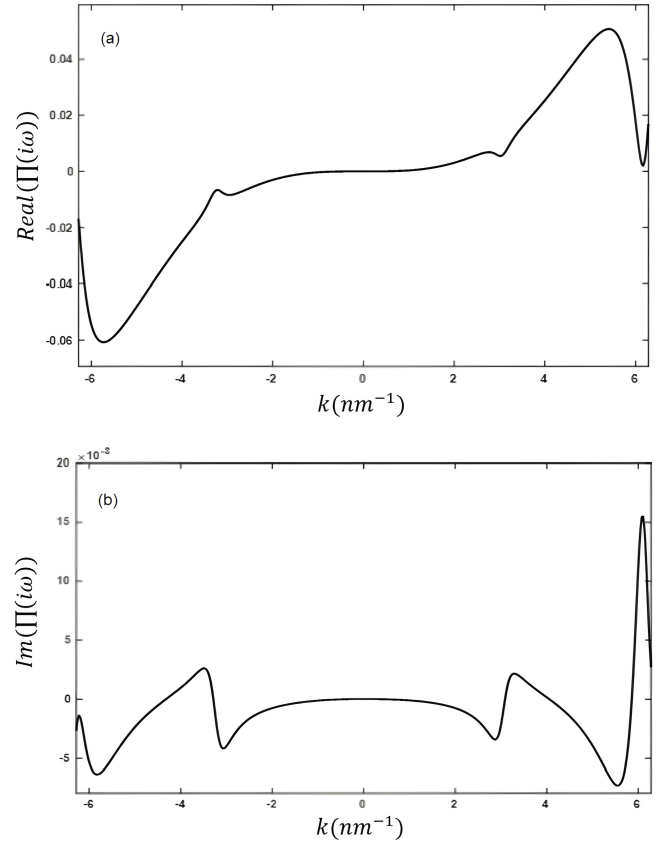


FIG. 4: (Color online) Panel(a), real part of the polarization of the Li_2IrO_3 as a function of k at T=10 K and for $q = 0.2nm^{-1}$. Panel (b) the corresponding imaginary part at the same conditions.

models hosting gapless and gapped QSL ground states²⁵. The magnetization data strongly confirm the dominance of the Kitaev-type ferromagnetic correlation and the vicinity of $\beta - Li_2IrO_3$ to the Kitaev spin liquid regime. Recent studies have established that $\beta - Li_2IrO_3$ is a highly promising candidate for the long-sought Kitaev spin liquid. Its anomalous magnetic properties result from its geometrical arrangement and strong spin-orbit coupling, which conspire to induce frustrated magnetic interactions. These results render $\beta - Li_2IrO_3$ a valuable focus of ongoing research on QSLs, with implications for advancing our understanding of quantum magnetism. With such fascinating properties, $\beta - Li_2IrO_3$ can pave the way for future studies and applications in quantum computing and other fields, a milestone in condensed matter physics. It is possible that the presence of other interactions, finite but small, marginally stabilizes a non-collinear order below $T_c = 38K$ ²⁶. The spectral function of the Kitaev-Heisenberg model is relevant to the investigation of the behaviors and properties of quantum spin systems. This model combines the Kitaev interactions, which are notorious for supporting Majorana fermions and topological properties, with the Heisenberg interactions that drive magnetic ordering.

The spectral function tells us about the excitation spectrum of the system, including how the energy levels are occupied and how they evolve under various parameters like temperature and external magnetic fields. Spectral function investigation is beneficial to researchers in examining the dynamics of quantum states, phase transitions, and emergent properties in these complex systems and is therefore a useful tool in theoretical and experimental condensed matter physics. Peaks in the spectral function in the Kitaev-Heisenberg model are crucial for comprehending the complex behaviors of quantum spin systems. It combines the Kitaev interaction, which creates strong frustration and leads to unconventional quantum states, with the Heisenberg interaction, which describes conventional magnetic coupling. The spectral function provides information on the energy distribution of excitations in the system, which reveals important features such as quasi-particle peaks and the presence of excitonic states. A study of these peaks in the spectral functions can also give further insights into the behavior of spin liquid phases and other emergent phenomena of quantum materials. The ongoing work on this subject continues to keep the interplay between all the interactions in the Kitaev-Heisenberg model at center stage, with the ability to lead to new breakthroughs in quantum magnetism and associated research fields. The spectral function comes into play to describe the density of states of a system across different energy levels. The spectral function is the Fourier transform of the regressive Green's function. The spectral function's peaks you see in the figure are energy levels at which particles such as electrons would be found to be. Studying the spectral function assists scientists in probing quantum state dynamics, phase transitions, and emergent phenomena in such complex systems and hence constitutes an effective tool for theoretical and experimental condensed matter physics. Peaks in the spectral function of the Kitaev-Heisenberg model are also central to explaining the complex behavior of quantum spin systems. This model complements the Kitaev interaction, which builds up strong frustration and leads to exotic quantum states, and the Heisenberg interaction, which is behind traditional magnetic coupling. The spectral function provides information on excitation energy distribution in the system, introducing prominent features such as quasi-particle peaks and the presence of excitonic states. The research of such peaks of spectral functions can assist in further advancing the knowledge of the nature of spin liquid phases and other emergent quantities in quantum materials. As research continues, the interaction competition in the Kitaev-Heisenberg model is still a central question, which can have the potential to reveal fresh insight into quantum magnetism and related fields. The spectral function describes a system's density of states at different energy levels. The spectral function is the Fourier transform of the regressive Green's function. The peaks in the spectral function that you notice from

the figure are energy levels where particles such as electrons are likely to be. The spectral function as a

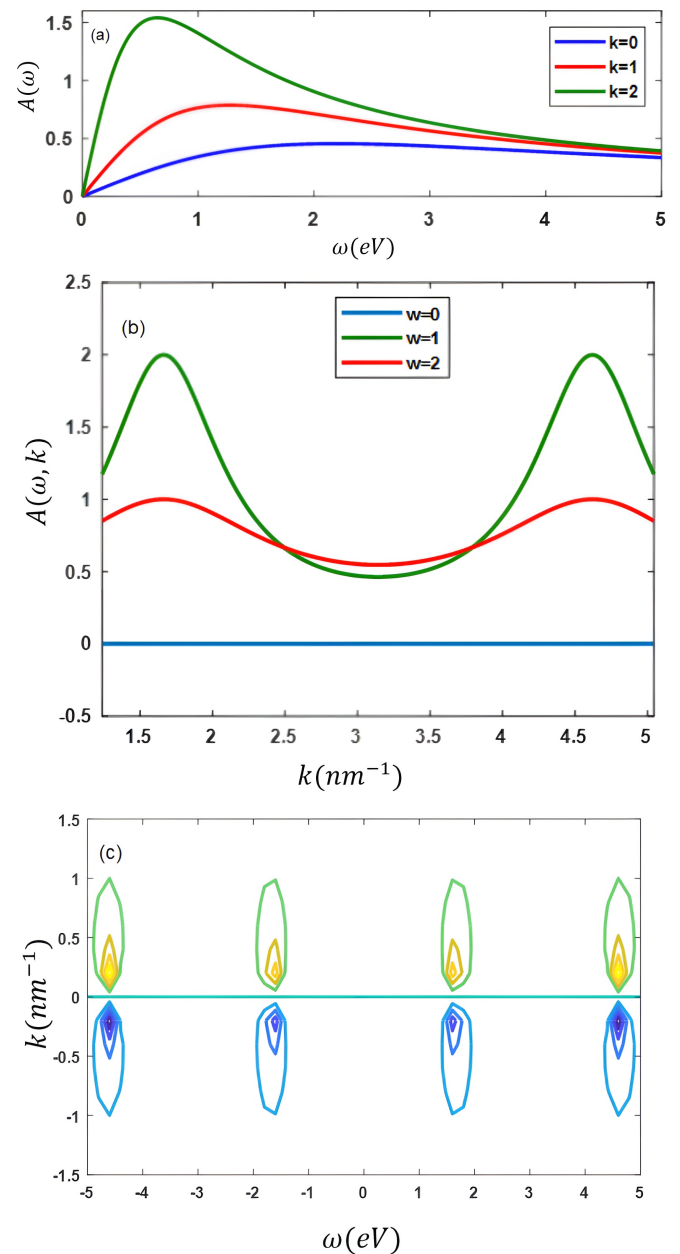


FIG. 5: (Color online) The spectral function of Li_2IrO_3 . The contour on the spectral function as a function of (a) ω , (b) k , and (c) the contour along k .

function of the extent of the K and ω is shown in Fig. 5. From the figure, there is one peak versus ω and two peaks versus K , other than when $\omega = 0$. The contour versus K is also plotted in Fig. 5. Bin-Bin Wang et al.²⁷ showed that in the zigzag phase, coherent quasi-particle features are exhibited clearly in spectral functions in the first Brillouin zone for holes created and annihilated on a sublattice, but they are hidden in physical spectral functions of angularly resolved optical emis-

Application	Advantage of Li_2IrO_3	Description
Quantum Spintronics	High SOC and no charge current	Efficient spin manipulation devices
Magnetic Sensors	Topologically protected edge states	High sensitivity, low thermal noise
Topological Memory	Quantum spin liquid background	Long coherence times
Majorana Devices	Non-superconducting, scalable architecture	Reduced fabrication complexity

TABLE I: Potential industrial applications of Li_2IrO_3 as a superconducting Majorana platform.

sion spectroscopy experiments such that these hidden spectral retrievals fall within extended Brillouin zones²⁷. Dynamical hole spectral functions provide rich information about the structure of fractional QSLs²⁸. The research revealed that the effective mass for fermionic quasi-particles like in $Ag_3LiIr_2O_6$ is, surprisingly, on the same order as the bare electron's effective mass²⁹. For the cuprate family, the effective mass increases with doping at approximately the same rate. This is consistent with the observed variation of effective mass in $(Sr_{1-x}La_x)_3Ir_2O_7$, which has a correspondence to the change in effective mass with doping in the iridates and this high-energy renormalization in the cuprates. This high effective mass in the metallic samples is on the order of, though a little higher than, values in a recent work in which the increase in mass was implied indirectly from infrared spectroscopy^{30,31}. The effective mass is

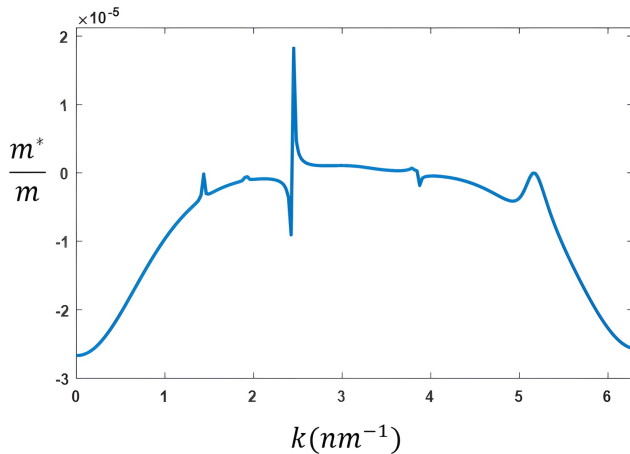


FIG. 6: (Color online) The effective mass of Li_2IrO_3 as function of k with $q = 5nm^{-1}$ and $T=10$ K.

graphed in Fig. 6 versus k , with its peak occurring at $k=2.4 nm^{-1}$. The charge carriers at the maximum of the effective mass have greater mobility, which leads to superior electrical conductivity and enhanced performance in semiconductor devices. Effective mass is the mass an electron or a hole effectively possesses when it reacts to forces, such as electric or magnetic fields, in a solid. The Kitaev-Heisenberg model's effective mass peak is a significant advancement in the quantum magnetism research, particularly for spin systems. The model adds the Kitaev interaction, which has the bond-dependent interactions and strong spin-orbit coupling, and the isotropic Heisenberg exchange interaction,

which includes the spin-spin coupling. The maximum of effective mass in this description is a remarkable point at which the character of the spin system alters, reflecting features of state degeneracy and topological order. Physicists use this description to investigate a broad range of quantum material phenomena involving quantum phase transitions and emergent excitations and yielding insights that can lead to new quantum computing and spintronic device applications.

IV. INDUSTRIAL APPLICATION

Li_2IrO_3 is a compound that exhibits fascinating magnetic and electronic properties, which makes it a hot subject in condensed matter physics. The Kitaev-Heisenberg model, when taken in the context of the material Li_2IrO_3 , gives significant industrial implications in the field of quantum computing as well as spintronics. The model with both Kitaev interactions and Heisenberg exchange leads to fascinating magnetic properties and exotic phases, e.g., Majorana-bound states. Li_2IrO_3 , a prime candidate in realizing such frameworks due to its remarkable electronic structure and high spin-orbit coupling, shows evidence of breaks in realizing quantum devices. The understanding and manipulation of Majorana modes from this Hamiltonian would pave the way towards fault-tolerant quantum computation because Majorana fermions are anticipated to be immune to external perturbations. Through investigating these industrial uses, scientists are not just pushing the limits of basic physics but also paving the way for future technologies that leverage quantum mechanics for everyday applications. Table I presents its industrial uses.

V. CONCLUSION

Our study puts Li_2IrO_3 on a realistic list of materials for the realization of superconducting Majorana fermions. The layer structure, spin-orbit coupling, and Kitaev interactions in combination offer a novel platform for future quantum technologies. Our proposal outlines the theoretical feasibility and industrial relevance of such systems. The real and imaginary parts of the polarization peaks play an important role in evaluating the magnetic properties and quantum states of the

materials. Numerical results showed that the sharp peak in the spectral functions indicates zero bias at the edges. The Kitaev-Heisenberg model is used to describe the magnetic properties. The geometric arrangement and strong spin-orbit coupling affect the magnetic properties of Li_2IrO_3 . The spectral function shows quasi-particle peaks and the presence of excitonic states. The results indicate that the charge carriers at the maximum effective mass have higher mobility.

VI. DECLARATION OF INTEREST

The authors declare that they have no known competing financial interests or personal relationships that could have appeared to influence the work reported in this paper.

* Electronic address: ghavamiba@gmail.com

- ¹ C. W. Beenakker, *Annu. Rev. Condens. Matter Phys.* **4**, 113 (2013).
- ² M. Leijnse and K. Flensberg, *Semiconductor Science and Technology* **27**, 124003 (2012).
- ³ T. D. Stanescu and S. Tewari, *Journal of Physics: Condensed Matter* **25**, 233201 (2013).
- ⁴ V. Kozii, J. W. Venderbos, and L. Fu, *Science advances* **2**, e1601835 (2016).
- ⁵ J. G. Rau, E. K.-H. Lee, and H.-Y. Kee, *Annual Review of Condensed Matter Physics* **7**, 195 (2016).
- ⁶ S. D. Sarma, M. Freedman, and C. Nayak, *npj Quantum Information* **1**, 1 (2015).
- ⁷ L. Savary and L. Balents, *Reports on Progress in Physics* **80**, 016502 (2016).
- ⁸ L. Clark and A. H. Abdeldaim, *Annual Review of Materials Research* **51**, 495 (2021).
- ⁹ L. Balents, *nature* **464**, 199 (2010).
- ¹⁰ M. Azizi and B. Ghavami, *RSC advances* **8**, 19479 (2018).
- ¹¹ B. Ghavami and A. Rastkar-Ebrahimzadeh, *Molecular Physics* **113**, 3696 (2015).
- ¹² A. Kitaev and J. Preskill, *Physical review letters* **96**, 110404 (2006).
- ¹³ Y. Kasahara, T. Ohnishi, Y. Mizukami, O. Tanaka, S. Ma, K. Sugii, N. Kurita, H. Tanaka, J. Nasu, Y. Motome, et al., *Nature* **559**, 227 (2018).
- ¹⁴ S. M. Winter, A. A. Tsirlin, M. Daghofer, J. van den Brink, Y. Singh, P. Gegenwart, and R. Valenti, *J. Phys.: Condens. Matter* **29**, 493002 (2017).
- ¹⁵ S. Trebst, arXiv preprint arXiv:1701.07056 (2017).
- ¹⁶ H. Takagi, T. Takayama, G. Jackeli, G. Khaliullin, and S. E. Nagler, *Nature Reviews Physics* **1**, 264 (2019).
- ¹⁷ E. Rostampour, B. Ghavami, S. A. Herrera, and G. G. Naumis, *Solid State Communications* **384**, 115497 (2024).
- ¹⁸ A. V. Chubukov and D. L. Maslov, *Physical Review B—Condensed Matter and Materials Physics* **86**, 155136 (2012).
- ¹⁹ D. D. Scherer, M. M. Scherer, G. Khaliullin, C. Honerkamp, and B. Rosenow, *Physical Review B* **90**, 045135 (2014).
- ²⁰ A. Toschi (2020).
- ²¹ A. Biffin, R. Johnson, I. Kimchi, R. Morris, A. Bombardi, J. Analytis, A. Vishwanath, and R. Coldea, *Physical review letters* **113**, 197201 (2014).
- ²² C. Kim, O. Vilella, Y. Lee, P. Park, Y. An, W. Cho, M. B. Stone, A. I. Kolesnikov, Y. Hao, S. Asai, et al., arXiv preprint arXiv:2502.14167 (2025).
- ²³ M. Kornjača and R. Flint, arXiv preprint arXiv:2410.21373 (2024).
- ²⁴ A. K. Bera, S. M. Yusuf, F. Orlandi, P. Manuel, L. Bhaskaran, and S. A. Zvyagin, *Phys. Rev. B* **108**, 214419 (2023).
- ²⁵ H.-D. Chen and Z. Nussinov, *Journal of Physics A: Mathematical and Theoretical* **41**, 075001 (2008).
- ²⁶ T. Takayama, A. Kato, R. Dinnebier, J. Nuss, H. Kono, L. Veiga, G. Fabbri, D. Haskell, and H. Takagi, *Physical review letters* **114**, 077202 (2015).
- ²⁷ B.-B. Wang, W. Wang, S.-L. Yu, and J.-X. Li, *Journal of Physics: Condensed Matter* **30**, 385602 (2018).
- ²⁸ W. Kadow, H.-K. Jin, J. Knolle, and M. Knap, *npj Quantum Materials* **9**, 32 (2024).
- ²⁹ J. T. Heath, F. Bahrami, S. Lee, R. Movshovich, X. Chen, F. Tafti, and K. Bedell, *Communications Physics* **6**, 348 (2023).
- ³⁰ G. Ahn, S. Song, T. Hogan, S. Wilson, and S. Moon, *Scientific reports* **6**, 32632 (2016).
- ³¹ W. Meevasana, X. Zhou, S. Sahrakorpi, W. Lee, W. Yang, K. Tanaka, N. Mannella, T. Yoshida, D. Lu, Y. Chen, et al., *Physical Review B—Condensed Matter and Materials Physics* **75**, 174506 (2007).